Available online at www.sciencedirect.com
SCIENCE DIRECT®

ELSEVIER

Tectonophysics 381 (2004) 211–233

TECTONOPHYSICS

www.elsevier.com/locate/tecto

Topography of the crust–mantle boundary beneath the Black Sea Basin

V. Starostenko[a], V. Buryanov[a], I. Makarenko[a,*], O. Rusakov[a], R. Stephenson[b], A. Nikishin[c], G. Georgiev[d], M. Gerasimov[e], R. Dimitriu[f], O. Legostaeva[a], V. Pchelarov[g], C. Sava[f]

[a] *Institute of Geophysics, National Academy of Sciences, Kiev, Ukraine*
[b] *Vrije Universiteit, Amsterdam, Netherlands*
[c] *Moscow State University, Moscow, Russia*
[d] *Sofia University, Sofia, Bulgaria*
[e] *Crimean Department of Ukrgeofizika, Simferopol, Ukraine*
[f] *Institute of Marine Geology and Geoecology "GeoEcoMar", Bucharest, Romania*
[g] *Geology and Geophysics Co., Sofia, Bulgaria*

Received 17 May 2001; accepted 8 August 2002

Abstract

A map of Moho depth for the Black Sea and its immediate surroundings has been inferred from 3-D gravity modelling, and crustal structure has been clarified. Beneath the basin centre, the thickness of the crystalline layer is similar to that of the oceanic crust. In the Western and Eastern Black Sea basins, the Moho shallows to 19 and 22 km, respectively. Below the Tuapse Trough (northeastern margin, adjacent to the Caucasus orogen), the base of the crust is at 28 km, whereas in the Sorokin Trough, it is as deep as 34 km. The base of the crust lies at 29 and 33 km depths respectively below the southern and northern parts of the Mid-Black Sea Ridge. For the Shatsky Ridge (between the Tuapse Trough and the Eastern Black Sea Basin), the Moho plunges from the northwest (33 km) to the southeast (40 km). The Arkhangelsky Ridge (south of the Eastern Black Sea Basin) is characterised by a Moho depth of 32 km. The crust beneath these ridges is of continental type.

Keywords: Black Sea; 3-D gravity modelling; Depth to Moho; Crustal structure; Geodynamics

1. Introduction

The Black Sea Basin (Fig. 1) is of paramount importance in providing a coherent geodynamic framework for the middle part of the Alpine–Himalayan orogenic belt and the adjacent southern margin of the East European Platform. The regional structure of the basin and the mechanisms that have controlled its evolution are, however, poorly understood and remain a subject of debate. Although it is generally considered to be a Cretaceous–Palaeogene back-arc basin related to subduction of an ocean since closed in present-day Turkey (Zonenshain and Le Pichon, 1986; Finetti et al., 1988; Artuyshkov, 1992; Golm-

* Corresponding author. Fax: +380-44-4502520.
E-mail address: irinam@igph.kiev.ua (I. Makarenko).

0040-1951/$ - see front matter © 2004 Elsevier B.V. All rights reserved.
doi:10.1016/j.tecto.2002.08.001

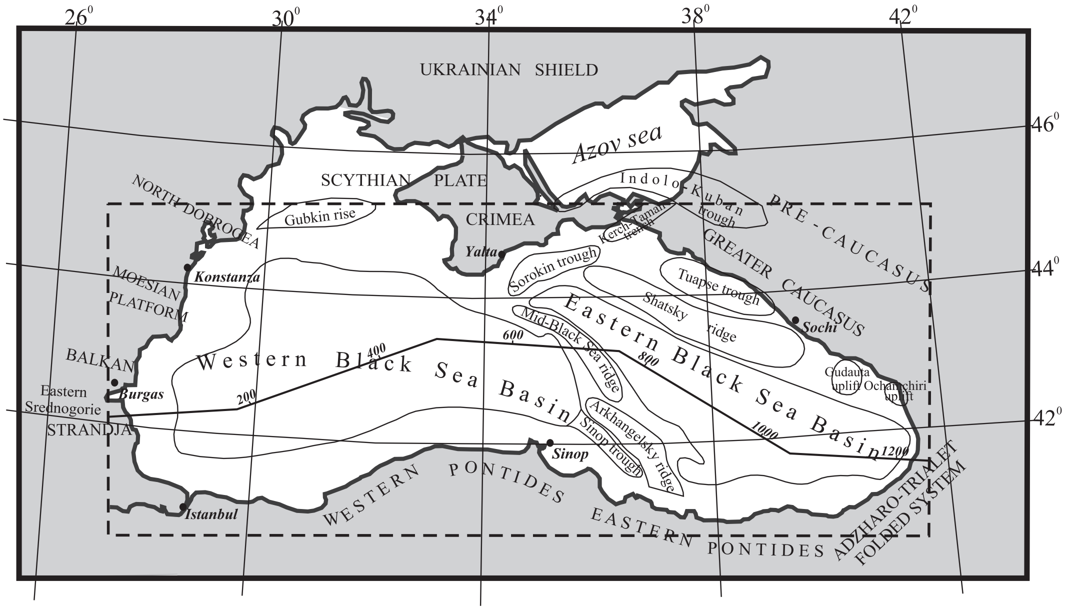

Fig. 1. Major tectonic features of the Black Sea region (after Tugolesov et al., 1985; Belousov and Volvovsky, 1992). Location of the modelled regional profile (Fig. 16) is shown by the solid line with distances marked. The dashed box delineates the area shown in subsequent figure.

stok et al., 1992; Dercourt et al., 1993; Okay et al., 1994; Gerasimov, 1995; Spadini et al., 1996; Robinson, 1997; Nikishin et al., 1997, Shnyukov et al., 1997; Georgiev et al., 2001), the internal structure of the basin is fairly complex. Not only are there the deep depressions floored by thin crystalline crust, but there are also shelf zones, uplifts (Mid-Black Sea and Shatsky ridges), troughs related to Late Cenozoic orogenic activity (e.g., Sorokin and Tuapse troughs), and a zone of complex geology between the Turkish Pontides and the deep basin.

As such, the geological history of the Black Sea Basin can be divided into the three major stages: (1) pre-Middle Cretaceous time, prior to the commencement of Black Sea opening; (2) a Middle–Late Cretaceous and/or in Palaeocene–Eocene phase of complex basin opening; and (3) post-rift development in Oligocene–Quaternary times, accompanied by orogenic activity in the surrounding areas such as the Greater Caucasus, Balkans, and Pontides. Any reconstruction of the regional kinematics of the Black Sea area must also take into account the mechanism responsible for the profound subsidence of the Western Black Sea Basin (16 km) since the Early Tertiary (Robb et al., 1998).

Thus, while there is general agreement about the back-arc nature of the Black Sea Basin, there is little consensus as to the age of the various tectonic elements, the position, number, and size of original Tethyan fragments, and, furthermore, in the utilisation of unified terminology for the region (e.g., Stephenson et al., 2001). These differences in opinion reflect the nuances of understanding of the regional geological history and hinder the development of a widely accepted geodynamic model for the basin. In this study, a preliminary attempt has been undertaken to arrive at reasonable compromise to various views.

The major tectonic elements in the basin are now viewed as a consequence of complex interactions between convergent and divergent processes. These interactions inexorably have resulted in density and thickness changes of the crust and upper mantle. It follows that any reconstruction of the geological history of the basin should predict the present-day mass (density) distribution. Even first-order constraints, such as on the depth to the base of the crust (inasmuch as these could help the estimation of extensional thinning parameters), can facilitate the appraisal of different scenarios for the tectonic development of the Black Sea.

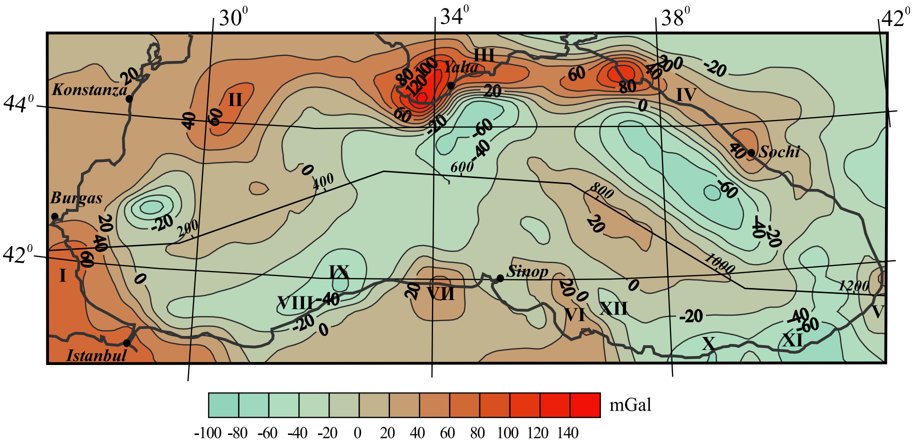

Fig. 2. Simplified anomaly gravity map of the Black Sea region: free-air anomalies (sea) and Bouguer anomalies (land). (I–XII) Local gravity anomalies mentioned in the text. Contour interval is 20 mGal. Location of modelled regional profile (Fig. 16) is shown by solid line.

Recently, detailed isopach maps for sediments of different ages, published previously as small-sized sketch maps (Tugolesov et al., 1985), have become available at a scale of 1:1,000,000. Additionally, new software, using such kinds of data, has been developed to enhance the resolution and interpretative capabilities of 3-D gravity modelling (Starostenko et al., 1997; Starostenko and Legostaeva, 1998) compared to earlier Black Sea gravity studies of much less resolution (Belousov et al., 1988; Yegorova et al., 1996). This has motivated the present study, a quantitative analysis of geophysical and geological data by 3-D gravity modelling of the Black Sea, aimed at inferring structure at the base of the crust and, in so doing, providing better insight into the regional and local tectonic history of the area.

2. The gravity field of the Black Sea

A composite gravity map of the Black Sea area (free-air anomalies at sea and Bouguer anomalies on land) is presented in Fig. 2. Its marine part is based on a 1:1,000,000 scale map compiled from about 35,000 observations (Fig. 3) made over about 40 years by various industrial and academic organisations from the former Soviet Union, including "Yuzhmorgeologiya", "Odessamorgeolo-

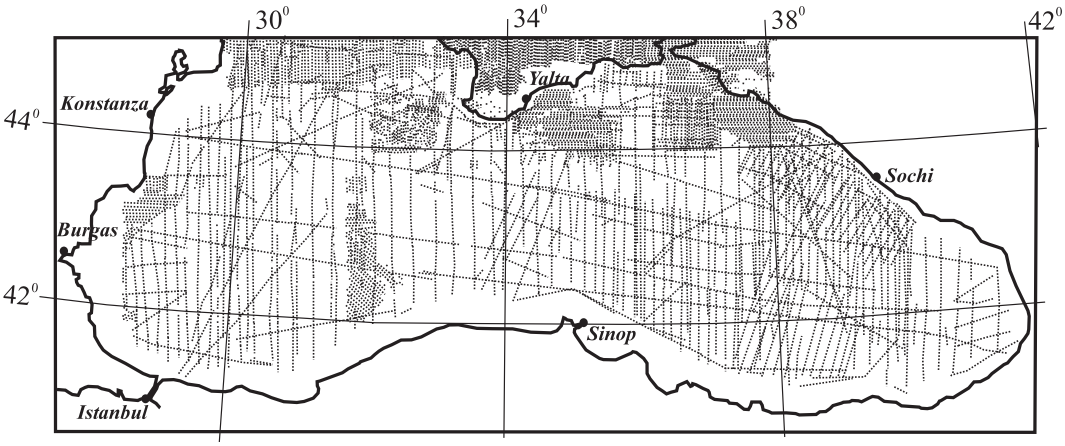

Fig. 3. Location of gravity measurements.

giya'', ''Yuzhmorneftegasrazvedka'', ''Vniigeofizika'', the Institute of the Physics of the Earth of the USSR Academy of Science, and the Institute of Geophysics of the National Academy of Science of Ukraine. Different instruments and navigation systems were used although all data have been reprocessed to a common standard and are referenced to IGSN71. The estimated free-air anomaly error is ± 1.6 mGal. The Bouguer anomalies (onshore part of Fig. 2) are from ZNIIGAiK (the Central Research Institute of Geodesy, Air Survey and Cartography of the former Soviet Union).

Despite a significant thickness of young, roughly flat-lying sediments in the Black Sea and their inferred more or less constant thickness (see below), there exist local positive and negative gravity anomalies within the basin with magnitudes of up to tens of milligals. Near the Bulgarian shelf (Fig. 2; east of Burgas), for example, there is a circular anomaly with individual observations as low as -85 mGal (<60 mGal at the scale and resolution shown in Fig. 2). The centre of another gravity low (observations as low as -90 mGal; <-60 mGal on Fig. 2), with sub-latitudinal strike, can be seen over the Sorokin Trough (Fig. 1, southeast of Crimea). A large gravity low of amplitude nearing -90 mGal strikes parallel to the Greater Caucasus coast. Near the eastern Anatolian coast, an offshore gravity low coalesces with the significantly negative gravity field of the Eastern Pontides.

Further, large amplitude, isolated gravity highs are observed on or near the margins of the Black Sea Basin and, except for the Gulf of Odessa (northwestern shelf), they extend onto land areas. Their marine termination nearly always coincides with the 200-m isobath. In the western sub-basin, two positive anomalies of 60–70 mGal occur (East Balkan and Burgas maxima; labelled I on Fig. 2) and cover the area from the western boundary of the Burgas zone to the West Pontides (Istanbul zone). On the boundary between the Black Sea Basin and the Gulf of Odessa, the Gubkinsky gravity maximum (II; Fig. 2) of about 100 mGal occurs (>60 mGal on Fig. 2). On the northern margin, there is a gravity maximum whose extreme value of over 180 mGal is associated with the Crimean Mountains (III). The large West Caucasus anomaly (IV; more than 100 mGal magnitude) is located on the northeast margin of the Black Sea; it begins on the shelf and then strikes along the coast to Sochi (Fig. 2). In the easternmost Black Sea, the Adjar positive anomaly (V) has a magnitude of more than 40 mGal. The southern margin (the Anatolian coast) is characterised by two positive anomalies (each with individual observations as great as 70 mGal). The first of these is situated southeast of Sinop (VI); the second to the west (VII).

There are also a number of gravity lows along the Anatolian coast, with amplitudes considerably larger than background values. These include anomalies VIII and IX, adjacent to the Western Pontides, and anomalies X and XI, the most negative anomalies in the Eastern Pontides, with observed values of -30 and -55 mGal, respectively. An unusual linkage is seen between the character of the gravity field and geological features on the central part of the Anatolian coast. Gravity high VI is associated with a trough with up to 4 km thickness of sediments (the Sinop Trough;

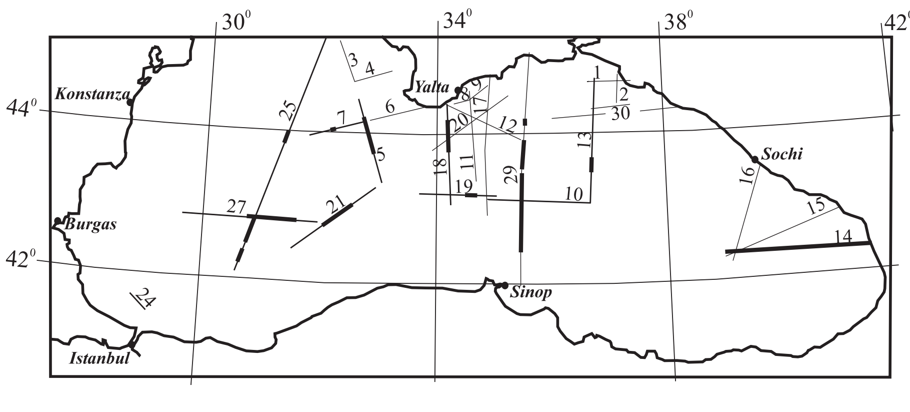

Fig. 4. Location of DSS profiles. Thickened lines indicate Moho depths directly controlled by refraction interfaces.

Fig. 1) whereas the associated gravity low (XII) coincides with a basement uplift (Archangelsky Ridge; Fig. 1).

In adjacent continental areas (not seen in Fig. 2), the gravity field shows a correlation with the deep structure of individual geological features: The Pre-Caucasus is characterised by small negative values; the Indol-Kuban Trough, Caucasus, Western and Eastern Pontides are dominated by a negative gravity field; in the Strandja zone, Eastern Srednogorie, East

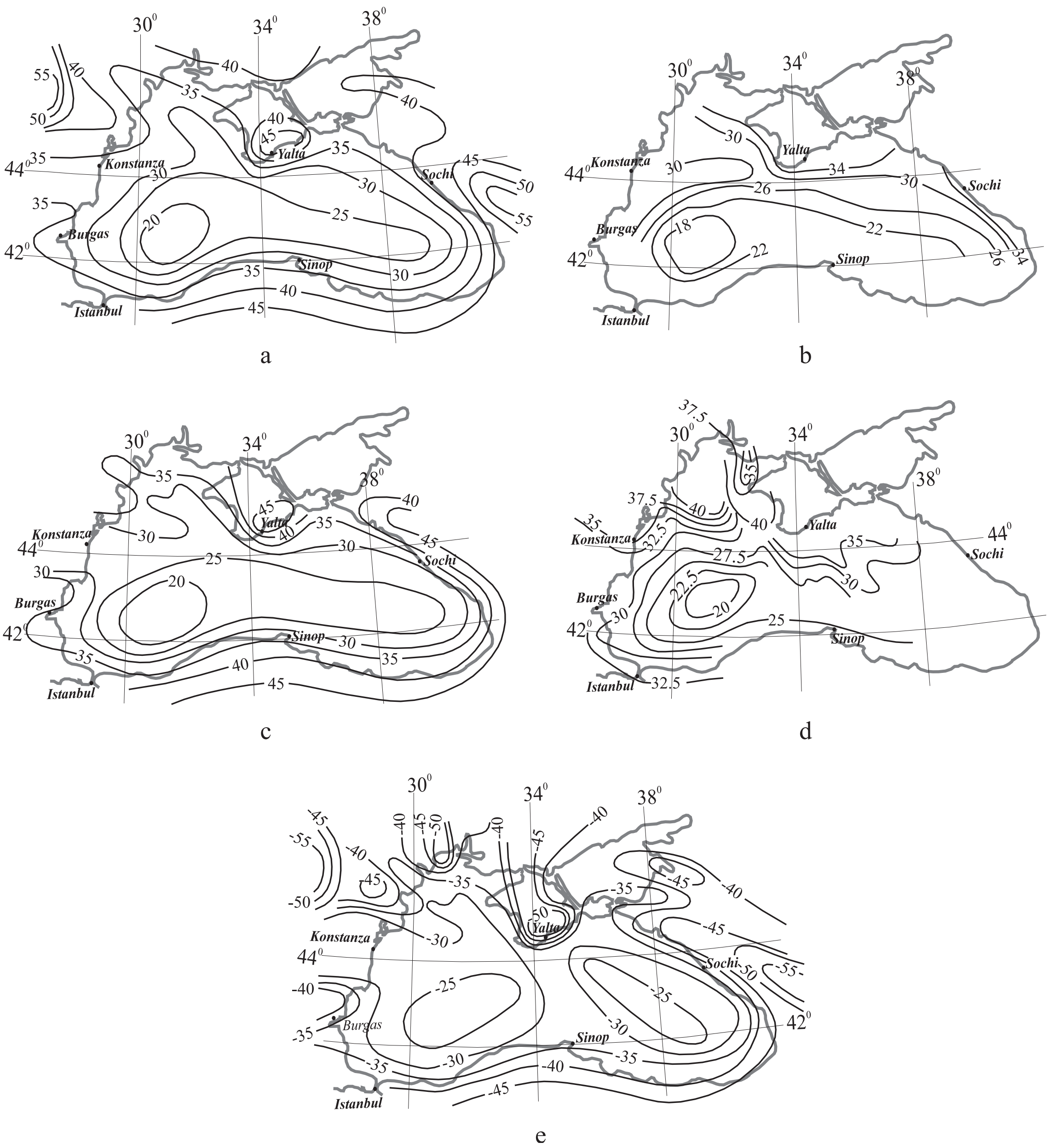

Fig. 5. Sketch maps of Moho depths: (a) after Balavadze et al. (1975); (b) after Neprochnov (1980) following Bulanzhe et al. (1975); (c) after Chekunov et al. (1992) following Bulanzhe et al. (1975); (d) after Sollogub (1986); (e) after Belousov and Volvovsky (1992).

Balkans, and on the Moesian Platform, the field is positive with relatively small amplitudes.

3. Crustal and supracrustal structure from seismic studies

Seismic data have been acquired in the Black Sea since 1957 (Tugolesov et al., 1985; Finetti et al., 1988; Belousov and Volvovsky, 1989, 1992; Volvovsky and Starostenko, 1996). The Deep Seismic Sounding (DSS) profiles seen in Fig. 4 were acquired between 1957 and 1968, and they have a total length of about 24,000 km. Moho depth is controlled by PmP (Moho reflection) and refracted phases where profile lines are thickened in Fig. 4. The DSS coverage is clearly not sufficient to give a reliable image of Moho topography but, nevertheless, a number of authors have compiled Moho depth maps for the Black Sea (Sketch map, 1970; Bulanzhe et al., 1975; Tugolesov et al., 1985; Sollogub, 1986); they are presented in Fig. 5. Given the sparse data, many tectonic structures within the basin are not recognised on these maps; for example, the Moho depth transition zone from sub-oceanic crust beneath the Black Sea to continental crust at its margins is only schematic, derived by interpolating widely spaced observations.

Thinning of the crystalline crust beneath the Black Sea is related to the "pinching out" of a "granitic" crustal layer and, consequently, significant shallowing of the Moho in the Western and Eastern Black Sea sub-basins, to 20 and 30 km depth, respectively. Beneath the Mid-Black Sea Ridge, the Moho lies deeper than 30 km. In a more recent study (Belousov and Volvovsky, 1992), crustal thickness is estimated to be 18–19 km at separate sites in the Western and 23 km in the Eastern sub-basins. The DSS data from the deep part of the basin consistently reveal a crustal velocity of 6.8 km/s (Bulanzhe et al., 1975), which may be interpreted as indicating oceanic crust.

The sedimentary layers within the Black Sea Basin have been studied in detail by multi-channel seismic reflection profiling along 140 regional lines with a total length of about 42,000 km. Line spacing is 20–25 km. The locations of seismic profiles used in the present study are shown in Fig. 6. The data utilised in

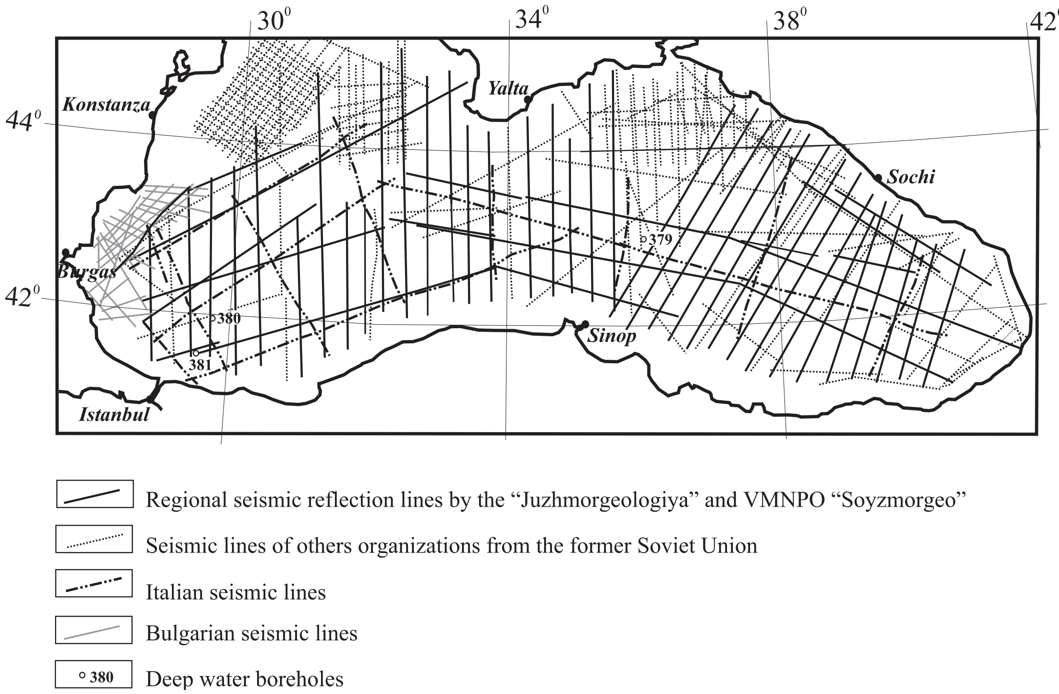

Fig. 6. Location of seismic reflection lines.

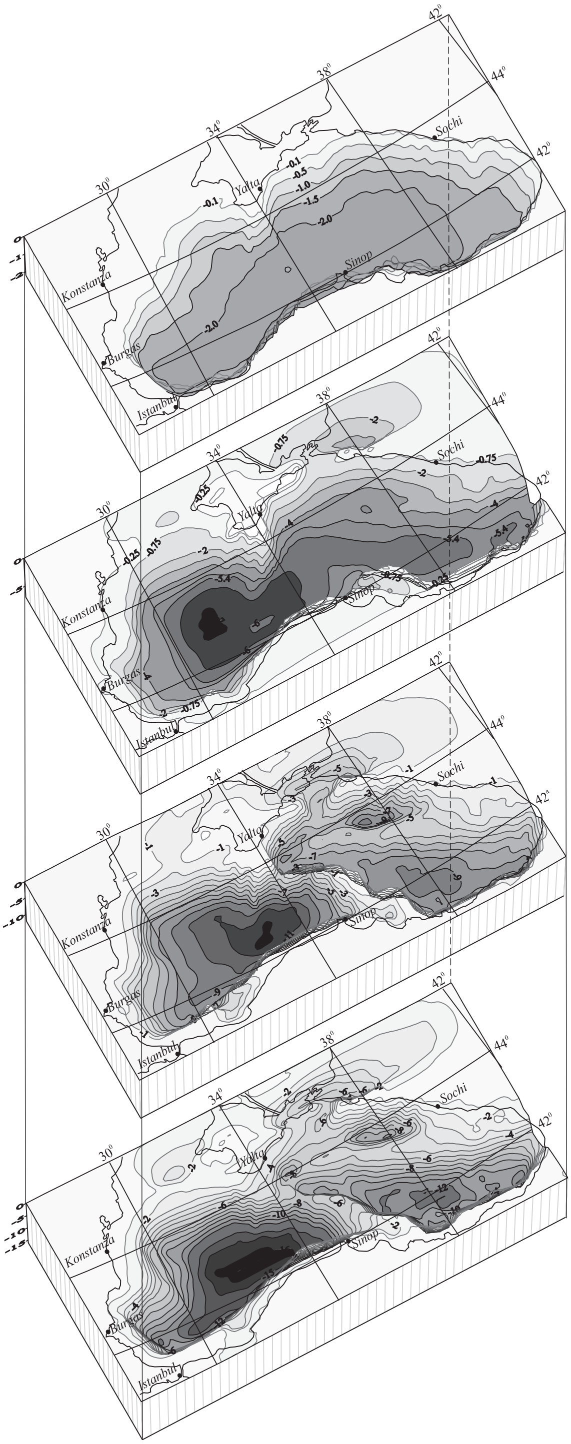

(a) Sea bottom topography

(b) Depth to the bottom of the unconsolidated sediments layer (top of the Maikop series)

(c) Depth to the bottom of the semiconsolidated sediments layer (top of the Eocene-Paleocene)

(d) Depth to the bottom of the consolidated sediments layer (top of the Mesozoic-Cainozoic)

Fig. 7. 3-D Structural model for the Black Sea basin. Units are in kilometres.

the present study have been summarised by Tugolesov et al. (1985) and Belousov and Volvovsky (1989). Three main sedimentary successions have been recognised as follows.

(1) The first (1–2 km thick), characterised by seismic velocities of 1.8–2.7 km/s, corresponds to upper Miocene–Pliocene–Quaternary sediments covering the whole of the floor of the Black Sea. This sequence was formed in post-Maikop time and is represented by interbedded sandy–clayish sediments deposited uniformly throughout the basin. It is separated from the underlying sediments by a distinct seismic boundary with velocity 3.0 km/s. The depth to the top surface of this succession (equivalent to the bathymetry of the Black Sea at the scale of the study) is shown in Fig. 7a and the depth to its base in Fig. 7b.

(2) The second succession (3–5 km thick) has velocities more than 3.0 km/s and is thought to correspond to lower Miocene sediments and the (Oligocene–lower Miocene) Maikop series. The depth to the base of this layer is shown in Fig. 7c. It is very thick, especially in the Sorokin and Tuapse troughs where it reaches a thickness of 4–5 km. It generally thins over the peripheral parts of the Black Sea floor. According to Chekunov (1990, 1992), these sediments record the formation of the East and West Black Sea sub-basins. However, recent seismic observations unambiguously show that underlying grabens are filled with Palaeogene sediments. In Oligocene–Neogene times, compressional deformation occurred in the foldbelts surrounding the Black Sea Basin. South-verging compressional features formed in sediments of this age in the Crimea–Caucasus zone and north-verging structures formed along the Turkish coast. However, this was not accompanied by uplift of the central part of the basin. Rather, the basin as a whole subsided rapidly during this time.

(3) The third and oldest sedimentary succession recognised from seismic observations in the Black Sea Basin, the base of which is shown in Fig. 7d, is 2–8 km thick and characterised by velocities of 4.5–5.0 km/s. It is interpreted to be mainly composed of Palaeocene–Eocene and, in places, Mesozoic (Cretaceous?) sediments. Palaeozoic and Triassic deposits are also occasionally represented in this layer. The thickness of Cretaceous deposits has been proposed to be 5–6 and 3–4 km in the Western and Eastern sub-basins, respectively. Their lithology is inferred from seismic data to be carbonaceous (Tugolesov et al., 1985). Palaeocene–Eocene carbonaceous and clayey sediments are 3–5 km thick.

Maps of the depth and thickness of these successions have been compiled by a number of authors (Tugolesov et al., 1985; Belousov and Volvovsky, 1989; Belousov and Volvovsky, 1992; Finetti et al., 1988; Ivanov, 1999). The thickest sediments are documented in the Western and Eastern Black Sea sub-basins (14 and 10 km, respectively). In the local Tuapse and Sorokin sub-basins, sedimentary cover is 8.5 and 7.5 km thick, respectively. A minimal thickness of sediments is observed above the Mid-Black Sea and the Shatsky ridges. In the axial parts of these structures, no Maikop and Eocene sediments occur whereas there are 3 km of Neogene–Recent deposits. Deposits of this same age have a similar thickness throughout the deep-water part of the basin.

Thus, in summary, three layers have been identified from seismic studies in the sedimentary cover. They are, in general: (1) the sub-horizontal sediments of middle Miocene–Recent age; (2) the Maikop series (Oligocene–lower Miocene) of the deep parts of the basin; and (3) the undivided syn- and post-rift sediments of the Cretaceous–Palaeocene–Eocene complex, which overlies either newly formed oceanic crust beneath the Western sub-basin or considerably thinned, probably heavily intruded by mafic material, pre-Cretaceous continental crust in the Eastern sub-basin (e.g., Nikishin et al., 1997).

4. Gravity modelling approach and model densities

4.1. 3-D Methodology and reference field

The 3-D methodology used to calculate the gravitational effect of the constituent geological elements of the Black Sea Basin and its underlying lithosphere includes a new approach to determining density contrasts and the reduction of calculated anomalies to a reference gravity field. It allows a quantitative way of estimating regional and local differences between observed and modelled gravity fields over large regions because all the component gravity contributions have been determined within a single reference system (cf. Appendix A).

All densities of the 3-D structural model are relative to the mantle density (3320 kg m^{-3}) immediately beneath the Moho of a tectonically stable Precambrian platform whose calculated gravity effect (g_{ref}) is -870 mGal, when the observed field is equal to zero (Fig. 8). The reduction of the calculated gravitational effect of the crust is constrained to this value. It is taken to be the zero level for the modelled field (cf. Appendix A). In fact, g_{ref} is partly a matter of convention, because its calculation depends on a number of assumed crustal parameters. Such an approach is mainly aimed at ascertaining density heterogeneities below the crust and was used, as an integral part of the methodology, in the "stripping" technique of Hammer (1963) to determine better the residual gravity effect of the mantle. The technique includes the successive calculation and removal of the gravity effects of individual supracrustal and crustal layers whose parameters are known. It was used in the present application to isolate the mantle gravity effect to allow modelling the topography of the crust–mantle boundary beneath the Black Sea Basin.

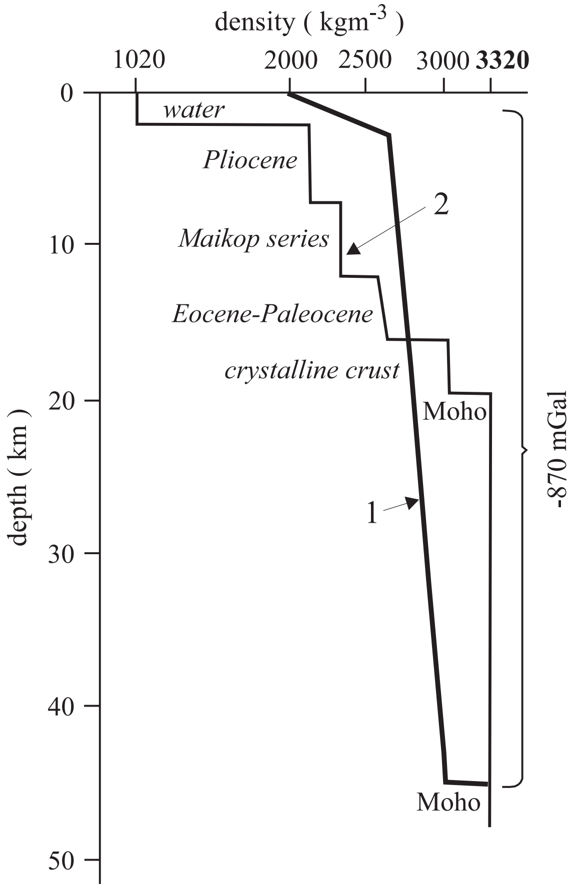

Fig. 8. Density versus depth in the crust of a Precambrian platform (1) and the Black Sea basin (2).

Gravity calculations were made using an automated method for the gravity study of 3-D layered heterogeneous media in which initial data (e.g., the observed gravity field, geometries of upper and lower surfaces of model layers and densities on these surfaces) take the form of simple maps (Oganesyan, 1987; Starostenko et al., 1997; Starostenko and Legostaeva, 1998). The method generalises the possibility of other kinds of software (see, for example, Götze and Lahmeyer, 1988; Starostenko, 1990) and has been applied previously to various geological targets (Yegorova et al., 1999; Dirkzwager et al., 2000; Yegorova and Starostenko, 2001). In the present study, computations were made on a regular grid of points generally spaced 20–25 km apart, increased to 50 km in areas of little variation in the gravity field and where sedimentary layer thicknesses are more or less constant. In total, 36 profiles each with 20 calculation points were obtained.

4.2. Density model

Accurate information on sediment density values within the deep part of the Black Sea Basin is extremely limited. Density measurements have only been made in the youngest sediments (Ross, 1978). Otherwise, averaged values of densities measured from samples of adjacent onshore areas as well as from general velocity/density relationships can be used.

There is only one published study of seismic P-wave velocity (V) versus density (ρ) for the sediments of the Black Sea region (Balavadze et al., 1975), obtained from samples of 1400 wells drilled in Western Georgia and the Kuban–Stavropol region of Russia (northeast of the Black Sea), and resulting in the following empirical relationship:

$$\rho = 1.8822 - 0.0871V + 0.1104V^2 - 0.0312V^3 \text{ kg m}^{-3} \quad (1)$$

Data from 17 wells drilled up to 4 km on the north-western shelf of the Black Sea are consistent with this relationship (Makarenko, 1997). Seismic velocities for the three sedimentary layers defined above have been converted into densities using this relationship and these are comparable to those determined from a large number of previously published data (cf. Table 1). The density contrasts of layers were obtained by subtraction the reference (upper mantle) density as described above:

$$\Delta\rho = (\rho_{\text{layer}} - 3320)\ \text{kg m}^{-3}$$

The resulting density model for sedimentary rocks in the Black Sea Basin, based on a water layer as well as the three sedimentary successions determined from seismic profiling as described in Section 3, is summarised in Table 1. The water density of 1020 kg m^{-3} for the Black Sea is based on comprehensive studies by Boguslavsky et al. (1980); from a depth of 500 m, the density does not exceed 1017 kg m^{-3}. The sedimentary layers (1–3) in the density model also include onshore segments representing sediments generally older than those of the equivalent Black Sea Basin succession.

The density adopted for consolidated sediments (layer 3) is 2600–2650 kg m^{-3}. This layer comprises (Cretaceous–) Palaeocene–Eocene deposits in the deep parts of the basin and Palaeozoic metamorphosed sediments in continental areas. The relatively high density is explained by the effects of burial, with densities reaching values comparable with those of crystalline rocks (Granser, 1987). For example, the average density of clays at depths of only 3000–5000 m measured on core samples from the Aralsor well (the Caspian region) is 2540 kg m^{-3} (Dortman, 1984). The density is 2630 kg m^{-3} in core samples (shales) taken from a depth of 1.8–2.0 km in Western Oklahoma (Athy, 1930). The Cenomanian carbonaceous formation of the Babadag Basin (the Romanian coast) has a density of 2650 kg m^{-3} (Dimitriu et al., 2000). On the other hand, terrigenous sediments are characterised by a density of 2570 kg m^{-3} at a depth of 3.6 km (Whitmarsh, 1979). In the Black Sea, seismic velocities of 4.5–5.0 km/s are observed at a 4–16 km depth.

A "granitic" crustal layer, comprising folded metamorphic complexes dating from the Archean to the Early Mesozoic in the study area, lies beneath the sedimentary layers in the density model. In the Black Sea Basin, this layer appears only at the margin of the deep basin. Its thickness gradually increases towards the coast line. Continental crust adjacent to the Black Sea is composed entirely of the "granitic" layer except for the uppermost 1–2 km of sediments. The physical characteristics of this layer are quite important, as they govern the gravity edge effect around the basin. DSS data, mainly from the Ukrainian Shield, indicate a seismic velocity of 6.5 km/s at a depth of 14–16 km, which is assumed to increase from 6.0 km/s at the surface giving a density range of 2600–2830 kg m^{-3}. The mean density of the "granitic" crustal layer in the density model is 2720 kg m^{-3}.

In the basin, two features are recognised from seismic data where a density "layer" taken to be the equivalent of the crustal "granitic" layer can be identified. The first is the Shatsky Ridge where the pre-Palaeocene basement occurs at a depth of 5.5 km

Table 1
Parameters of the 3-D density model for the Black Sea basin

	Layers	Age	Thickness, km	Average velocity, km s^{-2}	Literature* density interval, kg m^{-3}	Density interval deduced from relationship (1), kg m^{-3}	Adopted mean density, kg m^{-3}
	Water		up to 2	1.5	–	–	1020
1	Unconsolidated sediments	Pliocene–Quaternary	1–2	1.8–2.7	2000–2250	2010–2190	2150
2	Semiconsolidated sediments (Maikop series)	Oligocene–lower Miocene	up to 6	3.0–4.0	2260–2350	2260–2450	2350
3	Consolidated sediments	Paleocene–Eocene	2–8	4.5–5.0	2500–2660	2520–2570	2600–2650

*Balavadze et al. (1975); Belokurov (1976); Ross (1978); Neprochnov (1980); Bezverkhov (1988); Belousov et al. (1988); Makarenko (1997).

and at about 9 km an observed seismic boundary is interpreted as being the top of Jurassic sediments. The second one is the Mid-Black Sea Ridge, which is characterised by a velocity of 6.2–6.3 km/s (Bulanzhe et al., 1975). For both of these features, a density of 2720 kg m^{-3} is assumed.

The density of the "basaltic" sub-oceanic crust of the Black Sea Basin, the top of which lies at a depth of up to 16 km (cf. Fig. 7d), is taken to be 3040 kg m^{-3}. Density versus depth for a representative column in the Eastern Black Sea Basin—comprising water, the three sedimentary layers, a "basaltic" crustal layer, and mantle—for the adopted density model is shown in Fig. 8.

5. Gravity calculations

5.1. Gravity effect of water and sedimentary layers

The total gravity effect of the water layer (g_w) and the sedimentary cover (g_{sed}) is presented in Fig. 9. The greatest gradients are observed, as would be expected, on the Anatolian coast, south of Crimea, and on the northern Caucasus coast where the continental slope is the steepest. The greatest gravity effect occurs in the deep parts of basin where the sedimentary thickness is largest. It is more than −700 mGal in the Western Black Sea Basin and −560 mGal in the Eastern Black Sea Basin. Salients lie over the Sorokin (southeast of Crimea) and Tuapse (offshore Caucasus) troughs. The Mid-Black Sea Ridge, where the Cretaceous basement is only at a depth of 5–6 km, is easily seen in Fig. 9; in contrast, the Shatsky Ridge is not strongly evident.

5.2. Gravity effect of (intruded) crustal bodies on the margins of the Black Sea

Positive gravity anomalies peripheral to the Black Sea Basin (labelled with Roman numerals in Fig. 2) have been extensively studied by Buryanov et al. (1996, 1997, 1998, 1999a,b). In general, these anomalies comprise a number of distinct local maxima and the associated gravity gradients indicate that their inferred sources are quite shallow, often immediately below the supracrustal sedimentary layer. In marine areas, these anomalies and, accordingly, their source bodies are associated with the continental shelf; one exception is anomaly VI, which lies partly over the continental slope. There is little direct relationship between the gravity anomalies and the mapped geology. Similar anomalies are found on the peripheries of other Tethyan seas, such as the northern coast of the Mediterranean Sea (Ryan et al., 1971), the Tallish uplift on the western coast of the South Caspian Basin (Artemyev, 1973), and the African coast of the Alboran sea (Bonini et al., 1973).

The results of Buryanov et al. (1997) have been adopted in order to determine the gravity effect (g_{intr}) and physical parameters related to the source bodies of the Black Sea peripheral gravity anomalies. The source bodies, approximated by 18 prisms, and their cumulative gravity effect is shown in Fig. 10. More detailed 3-D modelling studies (Buryanov et al., 1996, 1998, 1999a,b) of anomalies I (Burgas, Romanian

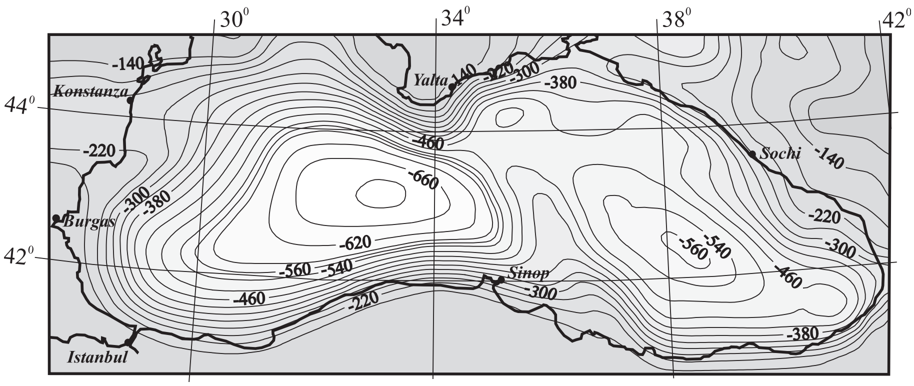

Fig. 9. Combined gravity effect of water and sedimentary layers. Units are in mGal.

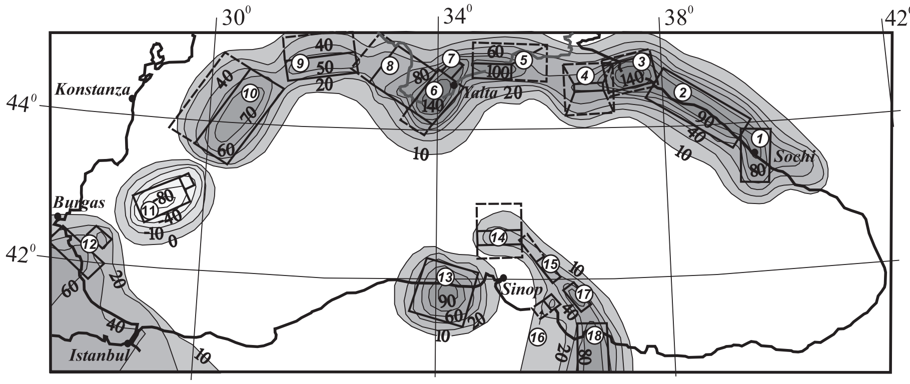

Fig. 10. The gravity effect of peripheral intrusions. Excess densities were calculated with respect to 2720 kg m^{-3} for the shelf and 2650 for Crimea–Caucasus zone. Units are in mGal. Parameters of model prisms (numbers) are listed in Table 2.

shelf), II (Gubkinskaya, Odessa shelf), III (Crimea–Caucasus), and VI (Sinop, Anatolian shelf) have also been taken into account. The gravity effect g_{intr} seen in Fig. 10 was computed with respect to a background density of 2720 kg m^{-3}, being generally characteristic of the upper part of the upper crustal layer on the shelf, except in the Crimea–Caucasus area where a density of 2600–2700 kg m^{-3} was used to a depth of 10 km (the density of the Crimean Tauriya series).

The geometry and densities of the source bodies are listed in Table 2. Their upper surfaces lie in the range 3.5–13 km depths, depending on the thickness of overlying sediments, but, as a rule, above the top of the crystalline crust. Maximum depths are as great as 30 km in the Eastern Black Sea Basin and 20 km in the Western Black Sea Basin and densities are in the range 2840–3320 kg m^{-3} (with the exception of body 11; Table 2), leading to their general interpreta-

Table 2
Parameters of the causative bodies of the peripheral gravity anomalies

Body	Anomaly	Upper edge		Lower edge		Density, kg m^{-3}
		Depth, km	Dimension, km	Depth to km	Dimension, km	
1	West-Caucasus (IV)	5	40 × 80	30	40 × 80	2890
2		5	50 × 190	30	50 × 190	2870
3		4	40 × 70	30	56 × 70	2940
4		3.5	10 × 40	30	70 × 75	2890
5		3.5	20 × 55	30	55 × 105	2920
6	Crimean Mountains (III)	3.5	69 × 70	30	101 × 70	2960
7		3.5	18 × 25	30	18 × 25	2970
8		13	44 × 70	20	44 × 90	2920
9		9	25 × 100	30	60 × 100	2840
10	Gubkinsky gravity maximum (II)	8	55 × 135	20	100 × 135	2920
11		5.5	42 × 70	7.5	42 × 70	2480
		7.5		20		2500
12	Burgas maxima (I)	3.5	30 × 80	20	30 × 80	2880
			20 × 30		20 × 30	
13		10	76 × 80	30	76 × 80	2870
14	Sinop Trough (VI)	13	20 × 63	19	80 × 63	2890
15		5	16 × 39	25	16 × 78	2920
16		5	16 × 20	25	20 × 36	2880
17		4	20 × 41	25	20 × 41	3020
18		5	50 × 81	25	50 × 81	2890

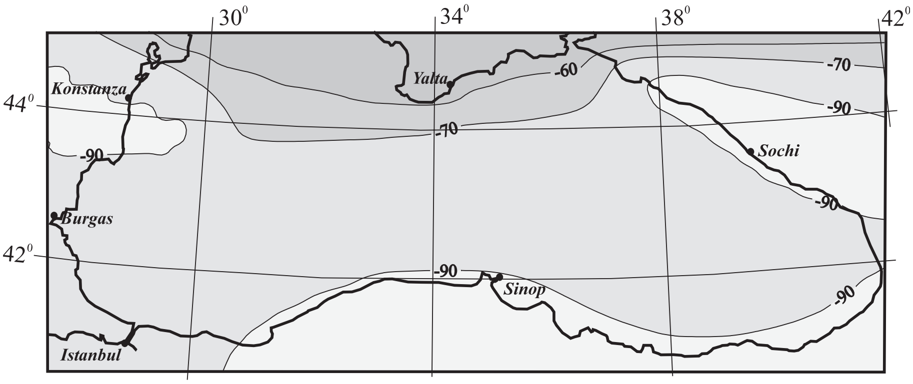

Fig. 11. The mantle component of the gravity field. Units are in mGal.

tion as mafic intrusions (Buryanov et al., 1996, 1997, 1998, 1999a,b).

5.3. Gravity effect of the mantle

The mantle component (g_m) of the gravity field of the Black Sea area obtained by Belousov et al. (1988) is show in Fig. 11. The inferred negative anomaly (~ -75 mGal) implies a mass deficit beneath the crust–mantle boundary in the deep part of the Black Sea, which can be explained in terms of higher than average mantle temperatures (Belousov et al., 1988).

One geotherm (temperature versus depth) that is compatible with the given g_m is shown in Fig. 12, where it is compared to that of the Precambrian platform. It was computed according to standard

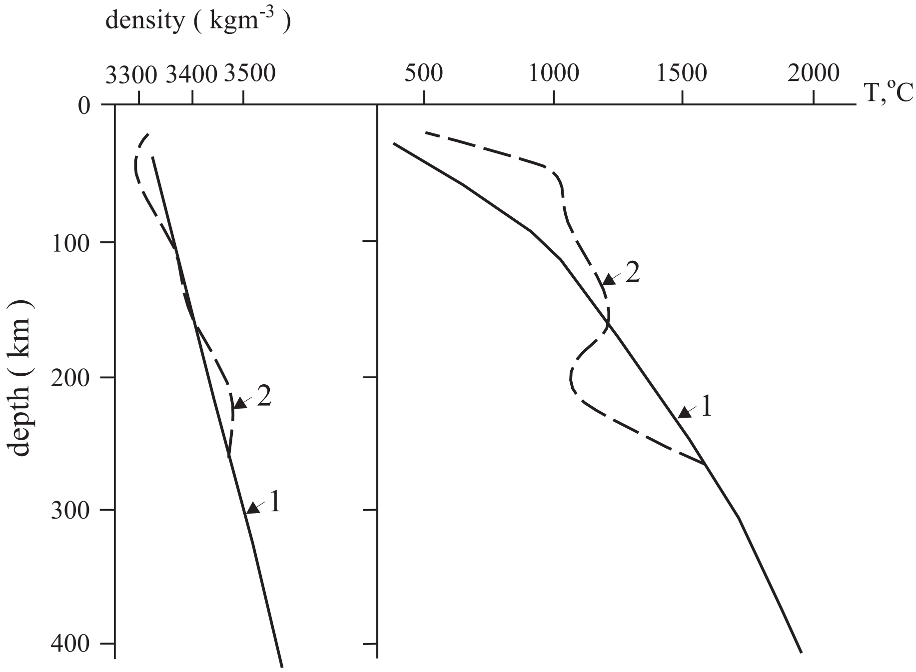

Fig. 12. Density and temperature versus depth in the lithosphere and sub-lithospheric mantle of a Precambrian platform (1) and the Black Sea basin (2).

Table 3
Parameters of the thermal model for the Black Sea basin

Layer	Thermal conductivity (W/mK)	Thermic diffusivity, (10^{-7} m^2/s)	Radiogenic heat generation, (10^{-6} W/m^3)	Density (kg m^{-3})	Age (m.y.)
Pliocene–Quaternary	1.09	2.00	0.84	1710	5.2
Middle–upper Miocene	1.26	4.50	1.13	1930	16.5
Oligocene–Miocene	1.59	6.40	1.56	2260	37.00
Paleocene–Eocene	2.76	8.42	1.56	2540	66.00
“Granitic”	2.68	12.75	1.59	2650	–
“Basaltic”	1.45	5.45	0.46	2950	–
Upper Mantle	2.76	11.45	0.03	3350	–

procedures (e.g., Carslaw and Jaeger, 1959), with physical parameters of lithospheric layers as listed in Table 3. The one-dimensional thermal model satisfactorily explains heat flow values observed in the Black Sea (about 150 measurements averaged in $1° \times 1°$ cells, later supplemented by an additional 500 observations, displaying averaged values in the range 40–60 mW m^{-2}) that were corrected for variations in submarine relief, long-period temperature fluctuations, convection (where known), and sedimentation effects (Kutas et al., 1998). Corresponding densities were calculated assuming a change of 10 kg m^{-3} with a temperature change of 100 °C (Bott, 1971). The density difference reaches -36 kg m^{-3} in the 25–160 km depth interval and is as great as $+27$ kg m^{-3} between 200 and 250 km, and this density profile produces a negative gravity anomaly of about -75 mGal in reference to the Precambrian cratonic lithosphere reference.

5.4. Residual gravity effect of the crystalline crust

The residual gravity anomaly generated by the crustal layer alone (g_{cc}), including the geometry of its base, is shown in Fig. 13. It is found by removing the gravity effects of the water and sedimentary layers (g_w and g_{sed}; Fig. 9), the peripheral intrusive rock bodies (g_{intr}; Fig. 10), and the mantle (g_m; Fig. 11) from the observed gravity field (g_{obs}; Fig. 2), i.e.:

$$g_{cc} = g_{obs} - (g_w + g_{sed} + g_{intr} + g_m - g_{ref})$$

Within the basin, the least negative gravity effect from the crystalline crust is observed in the Western and Eastern Black Sea basins (-120 and -220 mGal, respectively). The Mid-Black Sea Ridge and perhaps in part the Shatsky Ridge (cf. Fig. 1) are characterised by the most negative residual anomalies.

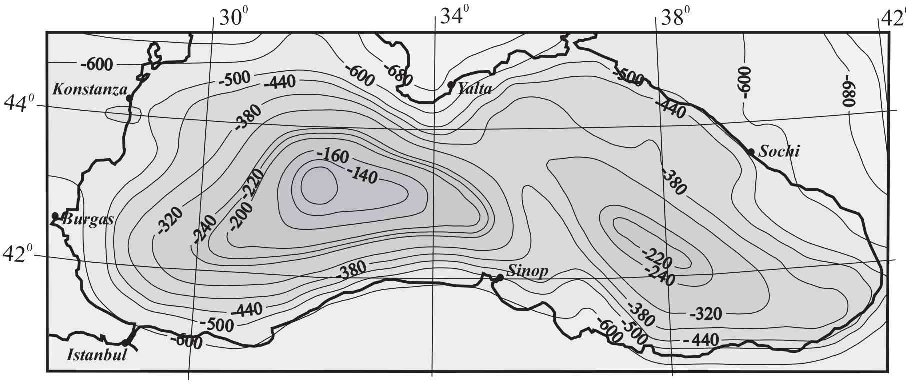

Fig. 13. The residual gravity field produced by the crystalline crust, obtained by removing the gravity effects of the water and sedimentary layers (Fig. 9), peripheral intrusions (Fig. 10), and the mantle component (Fig. 11) from the observed gravity field (Fig. 2). Units are in mGal.

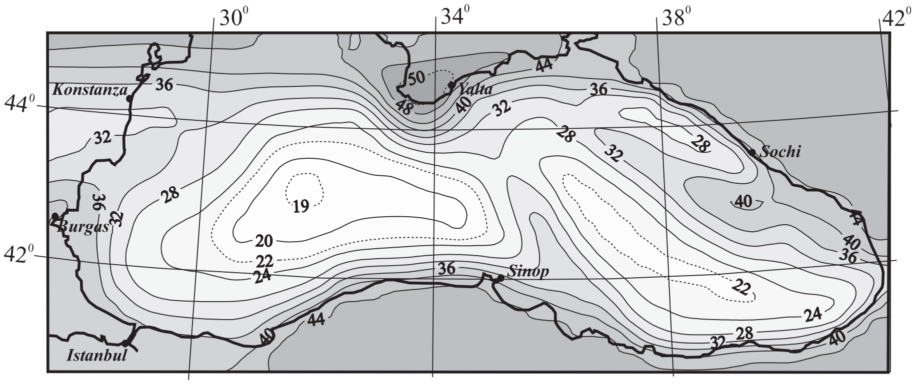

Fig. 14. Moho depths in the Black Sea Basin (km) as inferred from the interpretation of the gravitational response of the crystalline crust (Fig. 13). Units are in kilometres.

5.5. Model of the depth to the base of the crust (Moho geometry) and its uncertainty

The upper and lower surfaces of the crustal layer whose effect is shown in Fig. 13 are the basement surface and the Moho, respectively. Since the geometry of the basement surface is, in principle, known (cf. Fig. 7d), the geometry of the Moho can be found given the adoption of an appropriate density distribution in the layer. In practice, this was done in two steps, first, for the component of the crustal layer lying above a constant depth of 16 km, and then for the component lying deeper than 16 km, this depth being chosen because it is the maximum basement surface depth (cf. Fig. 7d). In the deepest basins of the Black Sea, the thickness of the crustal layer lying below 16 km can be assumed to be rather thin (based on the available DSS interpretations; e.g., Fig. 5). Furthermore, the crustal layer here appears to comprise only material of "basaltic" composition, with a seismic velocity of 6.8 km/s (Belousov and Volvovsky, 1992).

An initial density distribution in the crustal layer to 16 km ranging 2600–2840 kg m^{-3} from top to bottom (16 km) was adopted. The generally accepted density distribution for the "basaltic" of the Black Sea (2950–3120 kg m^{-3} from its top to its base) was adopted as the initial density distribution for the crustal layer deeper than 16 km. The resulting model, adjusted in order to fit the 3-D residual crustal gravity anomaly (Fig. 13), is summarised in terms of Moho depth and density of the crust deeper than 16 km in Figs. 14 and 15. In the final model, the lower crustal density in the Western and Eastern Black Sea basins is

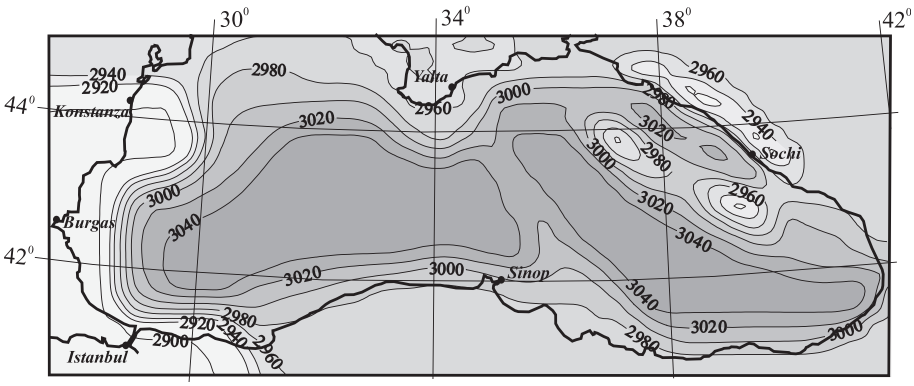

Fig. 15. Density distribution of the lower part of the crystalline crust for the best-fitting residual gravity model. Units are in kg m^{-3}.

3040 kg m^{-3}. Beneath, the Mid-Black Sea Ridge, where the top of the basaltic layer is known from seismic data to be at a depth of 18 km (Chekunov, 1994), a density of 3020 kg m^{-3} was adopted. Beneath the Shatsky Ridge and the Tuapse Trough the final model lower crustal density is 3000 kg m^{-3}, compensating for an even thicker upper crustal layer in these areas. On land, it is 2950–2970 kg m^{-3}, reaching its minimum on the Moesian platform (2900 kg m^{-3}) west of the Black Sea (Dachev, 1988).

Fig. 16 shows the final gravity model along the roughly east–west profile along the centre of the Black Sea (shown in Figs. 1 and 2), in which various elements of the gravity analysis are portrayed. For illustration purposes, the computed mantle gravity effect g_m is not included in the cumulative "residual anomalies" curve. The roughly constant separation of this curve with the observed gravity curve by g_m (~ -75 mGal) indicates the closeness of fit of model and observations.

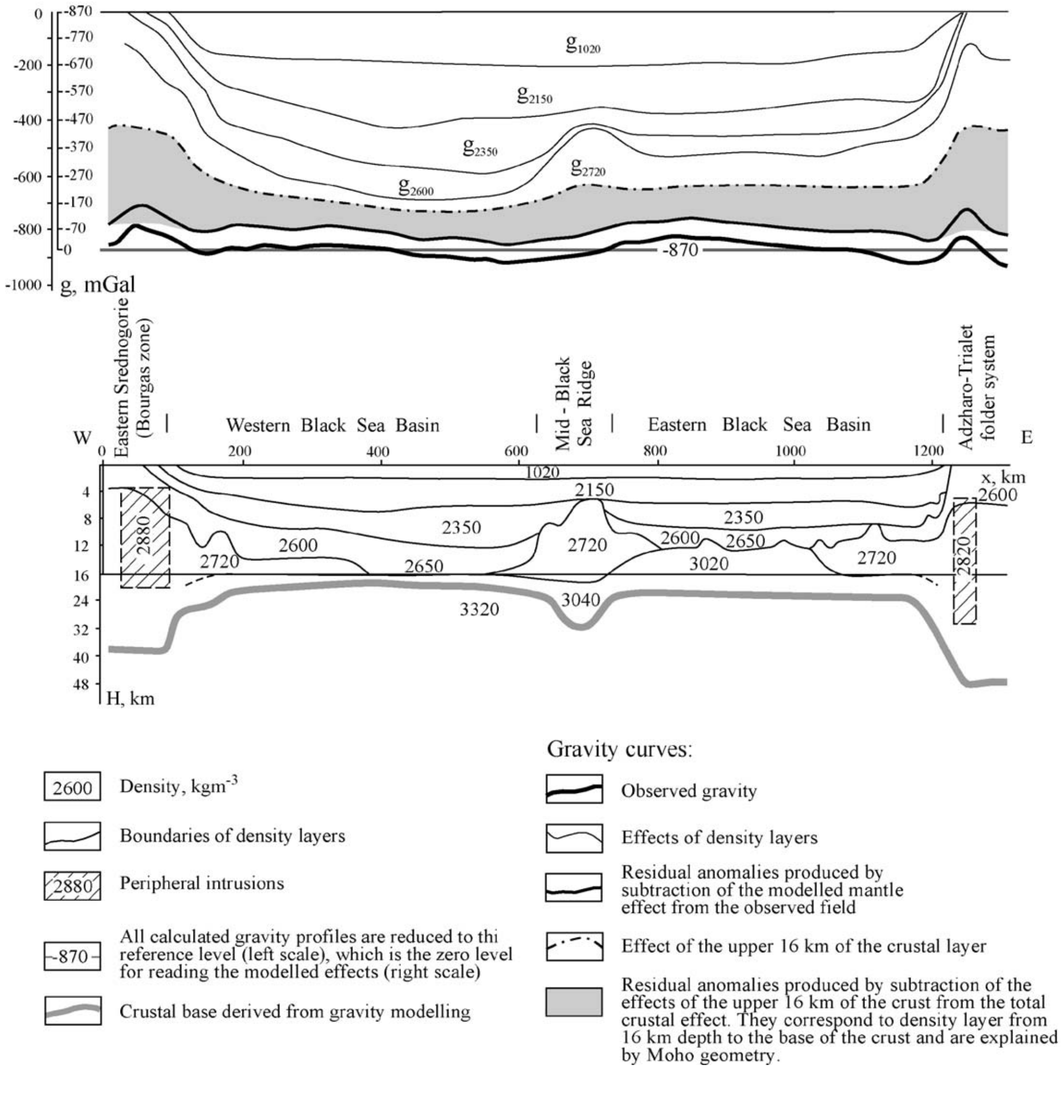

Fig. 16. Gravity model for the major tectonic features of the Black Sea (location profile is shown in Figs. 1 and 2).

It should be noted that the Moho depths in continental areas, within the study area, are more approximate than within the Black Sea because uncertainties having to do with adopted densities in the upper crustal "layer" (to 16 km depth) are much greater, as it is thicker and more variable. Indeed the calculated Moho depths in the peripheral continental regions are important mainly in defining the edge effect of continental crustal thickening on the gravity field.

The quality of final gravity model of Moho depth (Fig. 15) was assessed by comparing it to crustal thickness estimates based directly on seismic refraction interfaces where available. There are 33 pairs of such observations in the Black Sea. They gave a mean difference (neglecting sign) of 1.4 km with the standard deviation being about 2.5 km, comparable to uncertainties of Moho depths determined from DSS data in the western part of the Black Sea being $\pm 2-3$ km (Belokurov, 1976).

This level of uncertainty in the modelled Moho depths in the Black Sea compares with what might be expected from an analysis of errors associated with various steps in the procedure. Consider that the depths of sedimentary layer boundaries are accurate to ± 0.1 km and that the velocity–density conversion accuracy for sediments is ± 30 kg m^{-3}. A density variation of 50 kg m^{-3} in Eocene sediments at 11–16 km depth leads to an error in the gravity anomaly of 6 mGal. However, changing the depth to the boundary of a sedimentary layer by 0.1 km with a density contrast of 200 kg m^{-3} yields only a 3 mGal error. It follows that the gravitational response of water and sediments has been calculated with sufficient accuracy. Changes in the depth to the base of the crust by 1 km causes a change in gravitational response of 2 mGal on the continent and 25 mGal in the basin. Therefore, the accuracy of depth determinations can be estimated as being 1.5–2 km, comparable to what was inferred above.

6. Discussion

In the Black Sea Basin, the map of the depths to the base of the crust (Fig. 14) is much more detailed than those developed earlier from a limited number of DSS profiles (Figs. 4 and 5). The Moho map demonstrates a wide range of crustal thickness variation related to regional tectonic elements. In general, the base of the crust deepens more abruptly from the sea to the continent compared to the behaviour of the seafloor relief. In the Western Black Sea Basin, the crustal thickness gradient is less steep. On the boundary with the Scythian Platform (northwesternmost corner of the study area), this shallower gradient is caused by the effect of sediments associated with the Danube River (Tugolesov et al., 1985). Against the background of the general subsidence of the Black Sea Basin compared to surrounding continental masses, each large tectonic element has a distinct crustal thickness. The Moho is shallowest beneath the Western Black Sea Basin (19 km) and is somewhat deeper beneath the Eastern Black Sea Basin (22 km). The deepest Moho lies beneath the Shatsky Ridge (up to 40 km). In the Tuapse and Sorokin troughs, the depths to Moho are 28 and 34 km, respectively. Beneath the Mid-Black Sea Ridge, the base of the crust forms troughs of 29 and 33 km in the south and north, respectively. The deepening of the Moho in this region coincides with the uplift of the top of pre-Paleogene sediments.

The mean model depth to base of the crust for peripheral continental regions are 43–50 km for areas north of the Black Sea and Crimea (Scythian Platform and Ukrainian Shield); more than 50 km for the Crimean Orogen, southern Crimean peninsula; 37 km up to 42–45 km from the Indolo-Kuban Trough east to the Pre-Caucasus; 44 km in the vicinity of the western Greater Caucasus); 45–46 km in the Western and Eastern Pontides; 32–36 km in the Strandja and East Srednogorie-Balkan zone; and 31 km for the Moesian Platform. In general, these values do not significantly contradict those inferred from DSS profiles. For example, DSS results from Bulgaria suggest Moho depths of 30–32 km in the East Srednogorie–Balkan zone and 30–32 km in the Moesian Platform (Yosifov and Pchelarov, 1977; Dachev, 1988; Georgiev et al., 2001). The very deep Moho beneath southern Crimea could partly be artificial if the effects of dense intrusive rocks in the underlying crust have been overestimated (i.e., Section 5.2). However, a thick crust in this region is also observed on DSS models of the area (cf. Fig. 5).

In the Western and Eastern Black Sea basins, crystalline crustal thickness is characteristic of (sub-)

oceanic crust. The depth of the Moho beneath the Tuapse and Sorokin troughs, taking into account their thick sedimentary successions, suggests that the crustal layer is thinned continental crust and that it is of a transitional type adjacent to the thickened continental crust of the Crimean and Caucasus orogens. On the Shatsky Ridge, a decrease in lower crustal density in the final model (Fig. 15) suggests zones of coincident deepening of the basement surface. Both zones correspond with uplifts of Eocene sediments (Belousov and Volvovsky, 1989). The ridge is characterised by an intense positive magnetic anomaly (Alushta–Batumi zone; Kornev, 1982). Thus, the Shatsky Ridge, being the continuation of one of the Grater Caucasus massifs in Georgia according to Nikishin (in press), appears to have a mainly continental crustal affinity. The Arkhangelsky Ridge, on the southwestern margin of the Eastern Black Sea Basin, shows a thick continental crust and represents an uplift associated with extensional tectonics.

Finally, it should be noted that there are many local gravity anomalies, many of quite high magnitude, in the deep Black Sea basins that have not been addressed in the present study because of its resolution. These anomalies appear to be caused by dense rocks in the upper crystalline crust and, sometimes, apparently within the sedimentary layers, implying that they may be mafic intrusions. This interpretation is strongly supported by the general coincidence of positive magnetic anomalies with sources within the crystalline crust and, locally, in the sedimentary cover (Bulanzhe et al., 1975). The inferred intrusive bodies are so numerous in places that the upper crystalline layer displays a bulk seismic velocity as high as 6.8 km/s (Bulanzhe et al., 1975; Belokurov, 1976), similar to the lower crustal "basaltic" layer. Recent 2-D magnetic modelling (Yakimchuk et al., 1999), supported by gravity modelling (Buryanov et al., 1998; Yakimchuk et al., 1999; Stavrev and Gerovska, 2000) suggests that there are about 120 such bodies, occurring over a depth range of some 10 km throughout the whole Western Black Sea Basin.

7. Summary and conclusions

Gravity modelling in three dimensions, utilising all available seismic refraction/DSS and multichannel seismic reflection data for developing geological constraints, has allowed the construction of a new map of the depth to the base of the crust (Moho) in the Black Sea and immediate environs. The new map is more detailed than those previously available and, in effect, provides a quantitative interpolation of sparse observations of Moho depth in the Black Sea based on seismic studies.

In contrast to previously published models, the depth to Moho found in the present study increases abruptly from sea to land and shows a clear correspondence with see floor topography. Moho depth in the Black Sea ranges from 19 km in the Western Black Sea Basin to 40 km beneath the Shatsky Ridge.

All component tectonic elements of the Black Sea Basin display an inverse relationship between the thickness of the overlying sedimentary successions and that of the crystalline crust. Sedimentary thickness and the degree of crystalline crustal thinning are therefore controlled at least in part by a tectonic process, such as lithospheric extension. An oceanic crustal affinity is indicated beneath the main basin depocentres, based on crystalline crustal thickness. In contrast, the crust beneath Shatsky and Arkhangelsky ridges, on the northeastern and southwestern margins of the Eastern Black Sea Basin, is of continental type.

Bodies of high density are widespread on the periphery of the Black Sea Basin. They likely constitute ultra-basic and basic intrusions, formed during the main rift phase of the Black Sea Basin that began in the middle Cretaceous.

Acknowledgements

The authors are grateful to the journal's reviewers: S. Egan (University of Keele, Keele, England), I. Finetti (University of Trieste, Trieste, Italy), and J. Woodside (Vrije Universiteit, Amsterdam, Netherlands) for constructive criticism and valuable suggestions that significantly helped us to improve content and clarity of the manuscript.

Appendix A. Calculation of modelled anomalies

In any gravity model, two logically consistent facets are imperative. These are, first, the formation of density contrasts and, second, the reduction of the modelled field. In marine areas, where regional models are commonly derived, density differences are determined with respect to a sub-basin upper mantle density that is characterised by small positive and negative fluctuations. The mantle density is generally assumed to be in the range 3270–3400 kg m^{-3} (Rapolla et al., 1995) despite the uniformity of the gravity field (being near 0). Such a scatter in mantle density obviously can influence the amplitudes of computed anomalies produced by crustal sources.

This is illustrated in Fig. A1. A quantitative estimation of the error resulting from a mantle density discrepancy is made for a hypothetical local structure that simulates a typical submarine uplift. Adopted mantle densities of 3270 and 3400 kg m^{-3} respectively give calculated anomalies over the uplift of 165 and 140 mGal, after a graphic fitting of the tails of the gravity profiles. The discrepancy above the uplift is 25 mGal, which yields a $\pm$ 1 km error in determining the crust–mantle surface. By changing the parameters of the layers within the uplift and/or the mantle density below it, one can compensate for the mismatch. The crustal effects for basins adjacent to a submarine uplift with mantle density of 3270 and 3400 kg m^{-3} are -600 and -650 mGal, respectively. If these are taken as a zero level for each gravity profiles, the difference over the uplift comes to 75 mGal (i.e., $g_{m1} = -435$ mGal and $g_{m2} = -510$ mGal), fully three times larger than those graphically obtained.

This clearly demonstrates that the graphic technique of reducing a modelled field does not allow a true quantitative estimation of local density perturba-

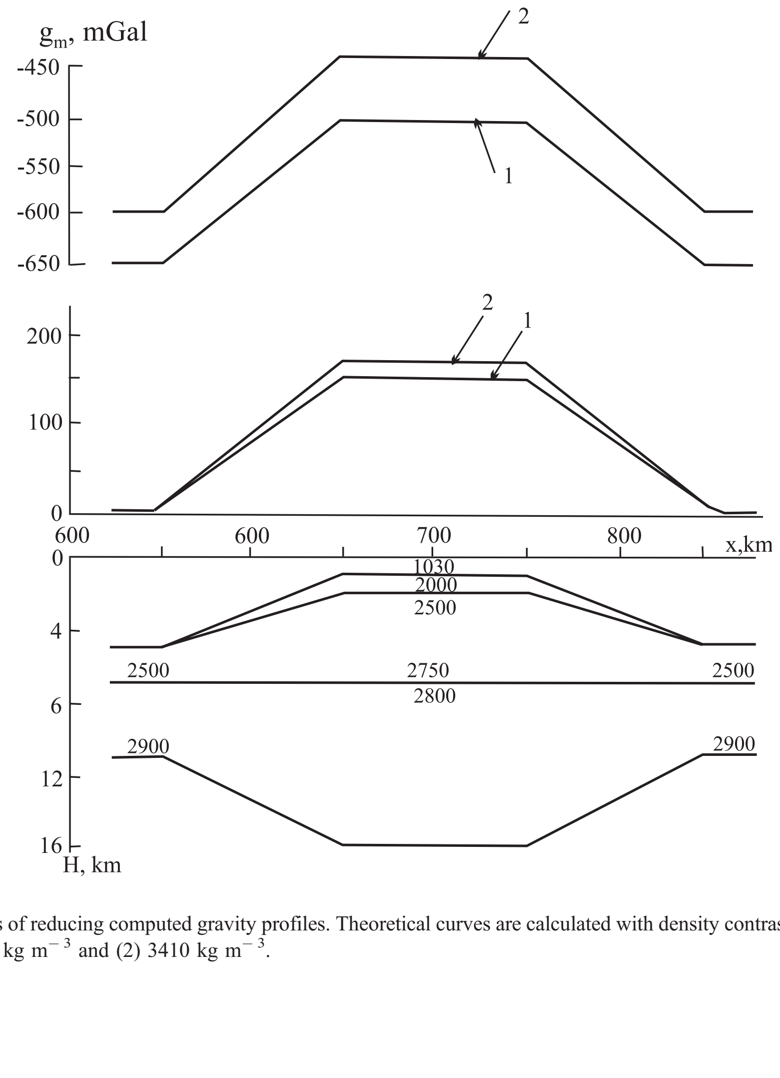

Fig. A1. Two realisations of reducing computed gravity profiles. Theoretical curves are calculated with density contrasts determined relative to a mantle density (1) 3270 kg m^{-3} and (2) 3410 kg m^{-3}.

tions nor discrimination of regional density inhomogeneities below the crust.

Worzel and Shurbet (1955a) were first to propose an approach for unifying the definition of density contrasts and reduction of modelled anomalies. They summarised what was known of oceanic and continental structure and derived "standard columns" for each (Fig. A2a,c). They differ from seismically based density sections in having two specific features. First, their geometries are slightly changed for the sake of simplicity. Second, in order to obtain the zero level of the gravity field over the sections, the thickness of their crystalline segments is also changed. Calculations using a 400 kg m^{-3} crust–mantle density contrast gave a density of 2840 kg m^{-3} for the crystalline layers, which is almost just the same as in more modern estimations. As both oceans and continents are very nearly in isostatic equilibrium, the mass per unit area for each standard column is therefore adjusted to be essentially the same. In this case, the gravitational attraction of each column is also the same. The calculation of gravity effects is therefore referred to these standard columns to obtain modelled anomalies.

The pioneering approach of Worzel and Shurbet (1955a) offered a new opportunity for broad interpretations of the gravity field independent of what crustal type was under consideration and this was amply demonstrated. Worzel and Shurbet (1955a,b), for example, were able to infer the very thin crustal section beneath ocean basins and successfully delineated the crustal transition zone at the Atlantic margin of the United States. Talwani et al. (1959, 1965) obtained new information on crustal sections crossing the Puerto Rico trench and the Mid-Atlantic Ridge. The standard column consisted of a 32-km-thick crust of density 2870 kg m^{-3} overlying a mantle of density 3400 kg m^{-3}. One key methodological result pointed out by Talwani et al. (1965, p. 349) was that: "The exact nature of the standard section is unimportant; what matters is the total mass down to a fixed level below which no lateral density inhomogeneities exist". By the middle 1970s, the concept of standard columns for gravity modelling of crustal structure was complete.

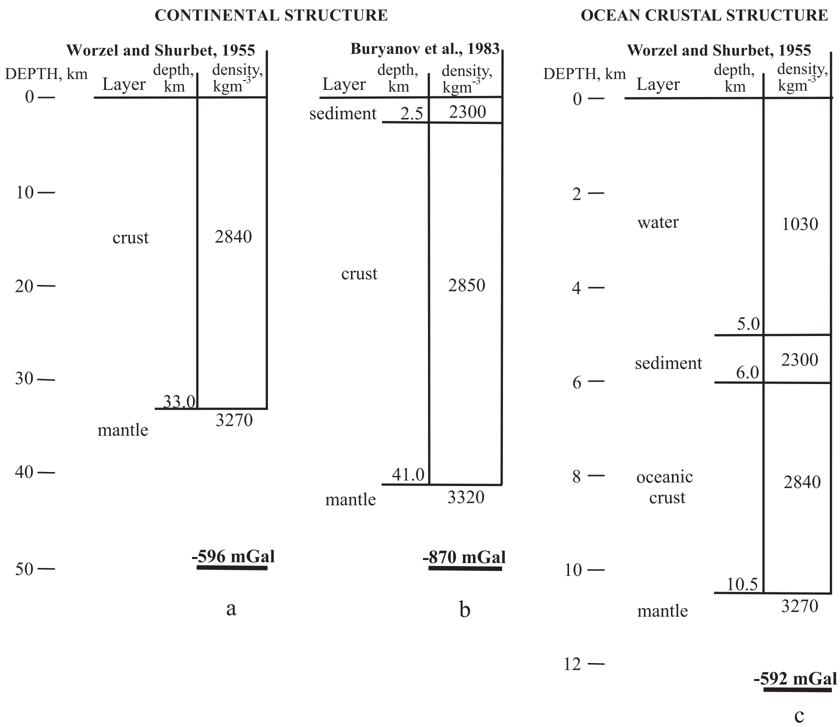

Fig. A2. Standard columns for reducing computed profiles in gravity modelling.

The first application of the standard column approach for estimating density perturbations in the upper mantle was by Segava and Tomoda (1974). Residual mantle anomalies near the Japan and Izu–Bonin arcs were explained in terms of a concentration of mass within the bending lithosphere due to possible elastic compression, phase transformations, or magmatic flows.

In the early 1980s, an important advance was made in applying the standard column method (Buryanov et al., 1983). These authors devised a genetic–statistical, rather than only statistical, method for constructing a standard section and a novel way of reading modelled anomalies. As a consequence the method became more transparent and easier to use, providing the opportunity to perform a true quantitative analysis of world-wide gravity modelling results.

As mentioned above, previous standard columns based on compiled seismic data were inferred from various continental or oceanic geological features having different origins and histories. The application of such a standard column, accordingly, involves fictitious gravity effects due to artificially "carrying" the specific characteristic of one class of geological features to another one.

To avoid this uncertainty, Buryanov et al. (1983) based their standard column on seismic observations from only stable and passive continental platforms. Their choice was justified by the global observation that only this class of geological feature had no density inhomogeneities in the crust and anomalous mantle. In contrast to previous works, therefore, it was no longer necessary to assume artificially an absence of lateral heterogeneities beneath some fixed level for constructing the standard column. On the other hand, a density cross-section of any crustal type is inexorably anomalous by comparison with those of a passive platform where no active thermal processes have occurred for a long time, probably since its origin.

The standard column based on data from a passive platform is shown in Fig. A2b. Density contrasts are produced relative to the mantle density beneath it:

$$\Delta\rho = \rho_{\text{layer}} - 3230 \text{ kg m}^{-3}$$

It follows that $\Delta\rho$ is always negative. The gravity effect of the standard column is equal to -870 mGal provided the observed field is zero. The reduction of calculated gravity anomalies is made in reference to this value, which is taken to be the zero level. Thus, any deviation from this reference level (g_{ref}) is a quantitative measure of density abnormality of layers under study relative to the standard column and beneath it.

The gravity effect of the mantle is

$$g_m = g_{\text{obs}} - (g_{\text{crust}} - g_{\text{ref}})$$

As all mantle components are obtained in a single system, they can be translated into a reasonable geological image by using an interdisciplinary approach. The practical application of gravity interpretation by the technique is illustrated in Fig. 15. Many successful examples this approach can be found elsewhere (e.g., Buryanov et al., 1983, 1985, 1987, 1997, 1999a,b, 2000; Belousov et al., 1988).

References

Artemyev, M.E., 1973. Isostasy of the USSR Territory Nauka, Moscow (in Russian).

Artuyshkov, E.V., 1992. Role of crustal stretching on subsidence of the continental crust. Tectonophysics 215, 187–207.

Athy, L.F., 1930. Density and porosity of sedimentary rocks. American Association of Petroleum Geologists Bulletin 14, 1–25.

Balavadze, B.K., Belokurov, V.S., Garkalenko, I.K., Malovitsky, Yu.P., Mindeli, P.Sh., Moskalenko, V.N., Neprochnov, Yu.P., Neprochnova, A.F., Starshinova, E.A., Chekunov, A.V., 1975. Physical properties of rocks Black Sea basin. In: Bulanzhe, Yu.D., Muratov, M.V., Subbotin, S.I., Balavadze, B.K. (Eds.), The Earth's Crust and the Black Sea Basin Evolution. Nauka, Moscow, pp. 254–269 (in Russian).

Belokurov, V.S., 1976. A complex geophysical zoning and some problems of the Black Sea basin tectonics. In: Bulanzhe, Yu.D. (Ed.), A Combined Study of the Black Sea Basin. Nauka, Moscow, pp. 11–21 (in Russian).

Belousov, V.V., Volvovsky, B.S. (Eds.), 1989. Structure and Evolution of the Earth's Crust and Upper Mantle of the Black Sea. Nauka, Moscow, 88 pp. (in Russian).

Belousov, V.V., Volvovsky, B.S. (Eds.), 1992. Structure and Evolution of the Earth's Crust of the Black Sea. Nauka, Moscow (in Russian).

Belousov, V.V., Volvovsky, B.S., Arkhipov, I.V., Buryanov, V.B., Evsyukov, Y.D., Goncharov, V.P., Gordienko, V.V., Ismagilov, D.F., Kislov, G.K., Kogan, L.I., Kondyurin, A.V., Kozlov, V.N., Lebedev, L.I., Lokholatnikov, V.M., Malovitsky, Y.P., Moskalenko, V.N., Neprochnov, Y.P., Ostisty, B.K., Rusakov, O.M., Shimkus, K.M., Shlezinger, A.E., Sochelnicov, V.V., Sollogub, V.B., Solovyev, V.D., Starostenko, V.I., Starovoitov, A.F., Terechov, A.A., Volvovsky, I.S., Shigunov, A.S., Zolotarev, V.G., 1988. Structure and evolution of the Earth's crust and upper mantle of the Black Sea. Bolletino di Geofisica Teorica ed Applicata 30 (117–118), 109–196.

Bezverkhov, B.D., 1988. Tectonics of the Mesozoic sedimentary cover in NW Black Sea as a basis for planning oil and gas exploration. PhD Thesis. Odessa University, Ukraine (in Russian).

Boguslavsky, S.G., Efimov, V.V., Cheresov, L.V., 1980. Combined Oceanographic Studies of the Black Sea. Naukova Dumka, Kiev (in Russian).

Bonini, W.E., Loomis, T.P., Robertson, J.D., 1973. Gravity anomalies, ultramafic intrusions and the tectonics of the region around the strait of Gibraltar. Journal of Geophysical Research 78 (8), 1372–1382.

Bott, M.H.P., 1971. The Interior of the Earth. Edward Arnold, London.

Bulanzhe, Yu.D., Muratov, M.V., Subbotin, S.I., Balavadze, B.K. (Eds.), 1975. The Earth's Crust and the Black Sea Basin Evolution. Nauka, Moscow, 358 pp. (in Russian).

Buryanov, V.B., Gordienko, V.V., Kulik, S.N., Logvinov, I.M., 1983. Integrated Geophysical Study of the Tectonosphere of the Continents. Naukova Dumka, Kiev (in Russian).

Buryanov, V.B., Gordienko, V.V., Zavgorodnyaya, O.V., 1985. A Geophysical Model for the Tectonosphere of the Ukraine. Naukova Dumka, Kiev (in Russian).

Buryanov, V.B., Gordienko, V.V., Zavgorodnyaya, O.V., Kulik, S.N., Logvinov, I.M., Shuman, V.N., 1987. A Geophysical Model for the Tectonosphere of Europe. Naukova Dumka, Kiev (in Russian).

Buryanov, V.B., Mankovsky, A.A., Solovev, V.D., 1996. The nature of gravity highs at the western border of the Black Sea (Burgas synclinorium). Geophysical Journal 16, 139–151.

Buryanov, V.B., Makarenko, I.B., Starostenko, V.I., 1997. Thickness and structure of the Black Sea Basin according to gravity modelling data. Geophysical Journal 16, 603–623.

Buryanov, V.B., Makarenko, I.B., Orovetsky, Yu.P., Starostenko, V.I., 1998. The geological origin of the Sinop tectonic junction in the South Black Sea region. Geophysical Journal 17, 583–602.

Buryanov, V.B., Makarenko, I.B., Orovetsky, Yu.P., Starostenko, V.I., 1999a. Geology of the Crimea–Caucasus gravity zone. Geophysical Journal 18, 1139–1152.

Buryanov, V.B., Makarenko, I.B., V.Legostaeva, O.V., Orovetsky, Yu.P., Starostenko, V.I., 1999b. The geological nature of the Radialnaya and Gubkinskaya gravity anomalies in the Western Black Sea region. Geophysical Journal 19, 153–168.

Buryanov, V.B., Gerasimov, M.E., Legostaeva, O.V., Makarenko, I.B., Rusakov, O.M., Starostenko, V.I., 2000. Preliminary models and comparison of the lower crust and upper mantle density patterns of the Black and Aegean seas. Geophysical Journal, Kiev 22 (4), 82–83.

Carslaw, H.S., Jaeger, J.C., 1959. Conduction of Heat in Solids. Clarendon Press, Oxford.

Chekunov, A.V., 1990. Problems of the Black Sea depression. Geophysical Journal, Kiev 4, 471–508.

Chekunov, A.V. (Ed.), 1994. The Lithosphere of the Central and Eastern Europe: Young Platforms and the Alpine Folded Belt. Naukova Dumka, Kiev, 331 pp. (in Russian).

Chekunov, A.V., Starostenko, V.I., Kozlenko, V.G., Koyfman, L.I., 1992. Contemporary views on geologic structure and evolution of the Black Sea basin. Problems of the Black Sea Intern. Oceanographic Commission, Sevastopol, pp. 197–208.

Dachev, Ch., 1988. Structure of Earth's Crust in Bulgaria. Technica Publ. House, Sofia (in Bulgarian).

Dercourt, J., Ricou, L.E., Vrielinck, B. (Eds.), 1993. Atlas Tethys, palaeoenvironmental maps. Gauthier-Villars, Paris, p. 307, 14 maps, 1 pl.

Dimitriu, R.G., Seghedi, A., Sava, C.S., Oaie, G., 2000. Geotectonic frame outlined by 3D interpretation of geophysical data in Danube delta region (Romania). Romanian Geophysics 7 (1), 114–117.

Dirkzwager, J.B., Stephenson, R.A., Legostaeva, O.V., 2000. The pre-Permian residual gravity field for the Dutch onshore and adjacent offshore. Global and Planetary Change 27, 53–66.

Dortman, N.D. (Ed.), 1984. Physical Properties of Rocks and Commercial Minerals (Petrophysics). Nedra, Moscow, 527 pp. (in Russian).

Finetti, I., Bricchi, G., Del Ben, A., Pipan, M., Xuan, Z., 1988. Geophysical study of the Black Sea area. Bolletino di Geofisica Teorica ed Applicata 30 (117–118), 197–324.

Georgiev, G., Dabovski, C., Stanisheva-Vassileva, G., 2001. East Srednogorie–Balkan rift zone. In: Ziegler, P.A., Cavazza, W., Robertson, A.H.F., Crasquin–Soleav (Eds.), Peri-Tethys Memoir 6: Peri-Tethyan Rift/Wrench Basins and Passive Margins, vol. 186. Memoires Museum National d'Histoire Naturelle, Paris, pp. 259–293.

Gerasimov, M.E., 1995. On geodynamics and presence of oil and gas in the Black Sea region. Geology of Oil and Gas 8, 4–11 (in Russian).

Golmstok, A.Ya., Zonenshain, L.P., Terekhov, A.A., Shainurov, R.A., 1992. Age, thermal evolution and history of the Black Sea based on heat flow and multichannel reflection data. Tectonophysics 210, 273–293.

Götze, H.-J., Lahmeyer, B., 1988. Application of three-dimensional interactive modeling in gravity and magnetics. Geophysics 53 (8), 1096–1108.

Granser, H., 1987. Three-dimensional interpretation of gravity data from sedimentary basins using an exponential density–depth function. Geophys. Prospect. 35, 1030–1041.

Hammer, S., 1963. Deep gravity interpretation by stripping. Geophysics 3, 369–378.

Ivanov, M.K., 1999. Focused heat flow on deep-water margins of the continents. PhD Thesis. Moscow State University, Russia (in Russian).

Kornev, O.S., 1982. Anomalies and structures of the Azov–Black Sea region. Geotectonics 3, 86–87 (in Russian).

Kutas, R.I., Kobolev, V.P., Tsvyashchenko, V.A., 1998. Heat flow and geothermal model of the Black Sea depressions. Tectonophysics 291, 91–100.

Makarenko, I.B., 1997. Earth's crust structure of the Black Sea Basin as inferred from gravity modelling. PhD Thesis. Institute of Geophysics, National Academy of Sciences of Ukraine, Kiev (in Russian).

Neprochnov, Y.P. (Ed.), 1980. Geology History of the Black Sea as

Obtained from the Results of the Deep-Water Drilling. Nauka, Moscow, 201 pp. (in Russian).
Nikishin, A.M., 2002. Tectonic history of the Black Sea basin. Bulletin MOIP (Moscow society of nature investigators), Department of Geology 3 (in press, in Russian).
Nikishin, A.M., Bolotov, S.N., Baraboshkin, E.Y., Brunet, M.-F., Ershov, A.V., Cloetingh, S., Kopaevich, L.F., Nazarevich, B.P., Panov, D.I., 1997. Mesozoic–Cenozoic history and geodynamics of the Crimea–Caucasus–Black Sea region. The Bulletin of the Moscow University, Geology 3, 6–16 (in Russian).
Oganesyan, M.G., 1987. Localization of the Sources and Solution of the Three-Dimensional Inverse Gravimetry Problems. PhD Thesis. Institute of Geophysics, National Academy of Sciences of Ukraine, Kiev (in Russian).
Okay, A.I., Sengor, A.M.C., Gorur, N., 1994. Kinematic history of the opening of the Black Sea and its effect on the surrounding regions. Geology 22, 267–270.
Rapolla, A., Cella, F., Dorre, A.S., 1995. Moho and lithosphere–astenosphere boundaries in East Africa from regional gravity data. Bollettino Di Geofisica Teorica Ed Applicata 37 (148), 277–303.
Robb, A., Nicolas, E.S., Williams, G., 1998. Integrated structural, sequence stratigraphic and geodynamic modeling of the Western Black Sea: early Mesozoic to recent. 3rd International Conference on the Petroleum Geology and Hydrocarbon Potential of the Black and Caspian Seas Area. Neptun-Constanta, Bucharest, Romania, 13–15 September, pp. 59–63 (abstracts).
Robinson, A.G. (Ed.), 1997. Regional and Petroleum Geology of the Black Sea and Surrounding Region. American Association of Petroleum Geologists Memoir, vol. 68, pp. 1–385.
Ross, D.A., 1978. Summary of results of Black Sea drilling. Initial Reports of the Deep Sea Drilling Project, vol. 42. Government Printing Office, Washington, US. Pt. 2, pp. 1149–1178.
Ryan, W.B.F., Sanley, D.J., Hersey, J.B., Fahrquist, D.A., Allan, T.B., 1971. Tectonics and Geology of the Mediterranean Sea. In: Maxwell, T.B. (Ed.), The Sea, vol. 4(II). Wiley, New York, pp. 387–492.
Segava, J., Tomoda, I., 1974. Gravity measurements near Japan and study of the upper mantle beneath the oceanic trench—marginal sea transition zone. In: Sutton, G.H., Manghnani, M.H., Moberly, R. (Eds.), The Geophysics of the Pacific Ocean Basin and its Margin. American Geophysical Union, Washington, pp. 35–52.
Shnyukov, E.F., Shcherbakov, I.B., Shnyukova, E.E., 1997. Paleoisland Arc of the Northern Black Sea. Chornobylinterinform, Kiev (in Russian).
Sketch Map of the Moho Relief Beneath the Black Sea and Adjacent Regions, Scale 1:2,500,000, 1970. Naukova Dumka, Kiev (in Russian).
Sollogub, V.B., 1986. The Lithosphere of the Ukraine. Naukova Dumka, Kiev (in Russian).
Spadini, G., Robinson, A., Cloetingh, S., 1996. Western versus Eastern Black Sea tectonic evolution: pre-rift lithospheric controls on basin formation. Tectonophysics 266, 139–154.
Starostenko, V.I., 1990. On: "application of three-dimensional interactive modeling in gravity and magnetics" (H.-J. Götze and B. Lahmeyer). Geophysics 55 (1), 116–117.
Starostenko, V.I., Legostaeva, O.V., 1998. Calculation of the gravity field from an inhomogeneous, arbitrarily truncated vertical rectangular prism. Izvestiya, Physics of the Solid Earth 34 (12), 991–1003.
Starostenko, V.I., Matsello, V.V., Aksak, I.N., Kulesh, V.A., Legostaeva, O.V., Yegorova, T.P., 1997. Automation of the computer input of images of geophysical maps and their digital modeling. Geophysical Journal 17, 1–19.
Stavrev, P., Gerovska, D., 2000. Magnetic field transforms with low sensitivity to the direction of source magnetization and high centricity. Geophysical Prospecting 48, 317–340.
Stephenson, R.A., Starostenko, V.I., Stovba, S.M., Rusakov, O.M., Kobolev, V.P., 2001. The enigma of the Black and Aegean seas evolution: a challenge to the geoscience community in the 21st century. Geophysical Journal 20, 787–792.
Talwani, M., Sutton, G.H., Worzel, J.L., 1959. A crustal section across the Puerto Rico trench. J. Geophys. Res 64 (10), 1545–1555.
Talwani, M., LePichon, X., Ewing, M., 1965. Crustal structure of the mid-ocean ridges: 2. Computed model from gravity and seismic refraction data. J. Geophys. Res. 70 (2), 341–352.
Tugolesov, T.A., Gorshkov, A.S., Meisner, L.B., Solov'ev, V.V., Khakhalev, E.M., 1985. Tectonics of the Meso-Cenozoic Deposits of the Black Sea Basin. Nauka, Moscow (in Russian).
Volvovsky, B.S., Starostenko, V.I. (Eds.), 1996. Geophysical Parameters of the Lithosphere of the Alpine Orogenic Belt. The Southern Sector. Naukova Dumka, Kiev, 215 pp. (in Russian).
Whitmarsh, R.B., 1979. The Owen Basin of the south-east margin of Arabia and the evolution of the Owen fracture zone. Geophysical Journal of the Royal Astronomical Society 58, 441–470.
Worzel, J.L., Shurbet, G.L., 1955a. Gravity interpretations from standard oceanic and continental crustal sections. In: Poldevaart, A. (Ed.), Geol. Soc. America Spec. Paper, pp. 87–100.
Worzel, J.L., Shurbet, G.L., 1955b. Gravity anomalies at continental margins. Proc. Nat. Acad. Sci. 41, 458–469.
Yakimchuk, M.A., Kobolev, Korchagin, I.N., V.P., Kozlenko Yu.V., Kutas, R.I., Soloviev, B.P., Zejgelman, M.S., 1999. Gravity and magnetic investigation in the Black Sea. EAGE 61st Conference and Technical Exhibition. Extended abstracts book, Abstracts 5–30, Helsinki, Finland, p. 4.
Yegorova, T., Starostenko, V., 2001. Large-scale 3-D density model for the lithosphere of Europe and Northeastern Atlantic. Geophysical Research Abstracts (EGS) 3, 58.
Yegorova, T.P., Kozlenko, V.G., Makarenko, I.B., Starostenko, V.I., 1996. A 3-D density model of the Earth's crust and upper mantle. In: Volvovsky, B.S., Starostenko, V.I. (Eds.), Geophysical Parameters of the Lithosphere of the Alpine Orogenic Belt. The Southern Sector. Naukova Dumka, Moscow, pp. 74–88 (in Russian).
Yegorova, T.P., Stephenson, R.A., Kozlenko, V.G., Starostenko, V.I., Legostaeva, O.V., 1999. 3-D Gravity analysis of the Dniepr–Donets Basin and Donbas Foldbelt, Ukraine. Tectonophysics 313 (1–2), 41–58.
Yosifov, D., Pchelarov, V., 1977. A scheme of the thickness of the Earth's crust in the Balkan Peninsula and some features of its structure. Geologica Balcanica 7 (2), 7–22 (in Russian).
Zonenshain, L.P., Le Pichon, X., 1986. Deep basins of the Black Sea and Caspian Sea as remnants of mesozoic back-arc basins. Tectonophysics 123, 181–211.